



# Fragile high capacity data hiding in digital images using integer-to-integer DWT and lattice vector quantization

Ehsan Akhtarkavan <sup>1,2</sup>  · Babak Majidi <sup>1,2</sup> · M. F. M. Salleh <sup>3</sup> · Jagdish C. Patra <sup>4</sup>

Received: 7 February 2019 / Revised: 27 November 2019 / Accepted: 3 January 2020

Published online: 29 January 2020

© Springer Science+Business Media, LLC, part of Springer Nature 2020

## Abstract

Data hiding in digital multimedia has been extensively used for sensitive data transmission and data authentication. An important property of data hiding which makes this method applicable to such applications is its fragility. The fragility is the loss of the embedded authentication credential resulting from any tampering attempt. Another important issue in data hiding and watermarking in digital images is increasing the embedding capacity while keeping the quality of the cover image high enough to avoid any perceptual degradation. In this paper a novel fragile digital image data hiding algorithm based on Lattice Vector Quantization (LVQ) is proposed to solve the above mentioned shortcomings. In the proposed data hiding algorithm after an initial pre-processing stage, the image is transformed into frequency domain using Integer-to-Integer Discrete Wavelet Transform (IIDWT). Then lattice vector quantization of  $A_4$  and  $Z_4$  lattices are used for embedding data into the cover image. The proposed embedding algorithm has the ability to hide the data inside the entire cover image. The experimental results show that the proposed data hiding algorithm performs significantly better than recently proposed algorithms when the embedding capacity is increased. At the high capacity regimes, the proposed algorithm can embed significantly more sensitive data in the cover image while keeping the perceptual quality of the recovered image high.

**Keywords** Watermarking · Data hiding · Digital image watermarking · Lattice vector quantization · Secure image communication · LVQ · Discrete wavelet transform

---

✉ Ehsan Akhtarkavan  
e.akhtarkavan@khatam.ac.ir

<sup>1</sup> Department of Computer Engineering, Faculty of Engineering, Khatam University, Tehran, Iran

<sup>2</sup> Pasargad Institute for Advanced Innovative Solutions, Tehran, Iran

<sup>3</sup> School of Electrical and Electronic Engineering, Universiti Sains Malaysia, Penang, Malaysia

<sup>4</sup> Faculty of Science, Engineering and Technology, Swinburne University of Technology, Melbourne, Australia

## 1 Introduction

In the past decade there has been a significant increase in the volume of data transferred digitally. The secure transmission of this data is of great interest for the scientific community. One method for secure transmission of digital data is hiding the data inside media files such as images, audio files and video files. The goal of digital data hiding in the images is to embed sensitive data inside a cover image with the condition that the original cover image along with the embedded data can be fully restored without any error. In order to protect the copyright of the digital multimedia such as movies and digital images it is possible to embed a hidden watermark inside the media. For example, for detection of the illegal distribution of early released movies the identity of the legal owner is embedded inside each distributed copy of the movie. If any illegally distributed copy of the movie is found, it would be possible to uniquely trace back the illegal copy to the exact owner of the early released movie. In Fragile data hiding algorithms any attempt to interfere with the cover media will result in damaging the embedded data which allows the receiving party to check the integrity of the data. The data hiding algorithm should also be able to keep the quality of the digital media as high as possible while embedding a significant amount of data inside the media.

The recently proposed algorithms are capable of robust data hiding with acceptable perceptual quality. However, there are three aspects which the data hiding performance can be improved with respect to recently proposed algorithms. The first aspect is that currently the performance of these data hiding algorithms and their embedding capacity are dependent on the content of the cover image. The second aspect is that the maximum embedding capacity with acceptable perpetual quality can be improved. Finally, the embedding stage in the above mentioned algorithms use variations of search methods for finding special blocks of pixels which are suitable for the embedding process rather than using the entire cover image.

The Lattice Vector Quantization (LVQ) has mainly been used for image compression [21, 34] and Multiple Descriptions Coding (MDC) [3, 5–8, 22, 55]. However, vector quantization can also be used for data hiding [40, 44–46]. In this paper, a novel fragile high capacity data hiding algorithm based on LVQ is proposed to improve the above-mentioned shortcomings. In the proposed scheme, first the image is transformed into frequency domain using the Integer-to-Integer Discrete Wavelet Transform (IIDWT). Then, the coefficients of the transformed image are lattice vector quantized. In this stage, an  $A_4$  lattice is used for the quantization process. The difference between the original frequency coefficients and quantized coefficients is calculated and the quantization errors are clustered. The clustered centroid are later used to improve the reconstruction of the cover image. The index of the centroid associated with every four pixels is added as the four most significant bits of the To-Be-Embedded (TBE) and two least significant bits are used for embedding the sensitive data. In the next stage based on TBE data bits, the mapped  $A_4$  sub-lattice point are re-quantized to the  $Z_4$  lattice point. Finally, the resulting image will be transformed back into the spatial domain using Inverse IIDWT. The experimental results show that the proposed data hiding algorithm is capable of performing significantly better than the recently proposed algorithms when the amount of TBE data in the images is high. The proposed algorithm can embed more data in the same cover images compared to other watermarking algorithms while keeping the quality of the cover image at an acceptable level of Peak Signal to Noise Ratio (PSNR) higher than 50 dB. For embedding capacities higher than 20 Kbits the proposed data hiding algorithm demonstrates higher perceptual quality in terms of PSNR. Also, this high capacity of embedding is consistent among many different cover images. Finally, the proposed data hiding algorithm has the ability

to hide the data inside the entire cover image and it is capable of extracting the embedded data without requiring the original image. The quality of the recovered cover image after extraction of the embedded data is very close to the condition of reversibility.

The rest of this paper is organized as follows. A review of the related works is provided in Section 2. The lattice vector quantization algorithm as well as the proposed data hiding algorithm is introduced in Section 3. The simulation study and the experimental results are presented in Section 4. Finally section 5 concludes the paper.

## 2 Related works

There are several methods for categorizing the digital image data hiding algorithms. It is possible to categorize the data hiding algorithms into transformed domain algorithms and spatial domain algorithms. Das et al. [16] proposed a new blind robust image watermarking in DCT domain which uses inter-block coefficient correlations. The proposed method uses homomorphic cryptosystem to achieve PSNR values close to 38 dB. The computational complexity of the proposed method is low compared to similar algorithms. Patra et al. [41, 42] proposed a method for digital image watermarking using Chinese remainder theorem. The proposed method is resistant to tampering. Shirafkan et al. [50] proposed a steganography scheme based on discrete wavelet transform using lattice vector quantization and Reed-Solomon encoding. Nguyen et al. [38] proposed an algorithm for watermark embedding using independent component analysis. Akhtarkavan et al. [2] proposed a high capacity watermarking algorithm for embedding the low altitude aerial data for secure transmission and archiving of the remote sensing information.

Gunjal et al. [23] proposed an algorithm for secure, robust and high capacity watermarking in DWT-SVD domain. The proposed algorithm uses half toning and simplified block truncation coding for data hiding in the images. In the proposed algorithm the maximum PSNR values is 64.35 dB and the average payload is 231,063.8 bits. The processing time for the proposed algorithm is 7.05 ms. The proposed algorithm is evaluated on the McGill and Osirix databases and it is concluded that it has advantages from robustness and capacity perspectives over other data hiding algorithms. Kalra et al. [28] proposed an adaptive digital image watermarking algorithm for data hiding in color images in frequency domain. The proposed algorithm uses the logistic map and hamming code in order to achieve PSNR values higher than 37 dB. The proposed algorithm is tested against various attacks and it is concluded that it is secure against VQ attacks.

In another approach the digital image data hiding algorithms are categorized into reversible or lossless algorithms and irreversible algorithms. Chang et al. [10] proposed a high capacity reversible data hiding algorithm which uses residual histogram shifting for block truncation coding. The maximum PSNR achieved using the proposed algorithm is 50.54 dB and the maximum payload is 41,194 bits. The proposed algorithm is compared with similar algorithms and it is concluded that the higher efficiency and payload can be achieved using the proposed method.

Weng et al. [58] proposed a new data hiding algorithm based on  $k$ -pass Pixel Value Ordering (PVO). The proposed algorithm is an effective reversible data hiding (RDH) technique. In the proposed algorithm, some pixels in a block are used with the neighborhood pixels surrounding the block for increasing the accuracy of local complexity. Then, the rest of

the pixels are used for improving the  $k$ -pass PVO using the location relationships. The proposed method achieves acceptable results when a large data is required to be embedded.

Digital image data hiding algorithms are also categorized based on the type of the cover image. The cover image can be compressed, uncompressed, or encrypted. Hossain et al. [25] proposed a blind watermarking algorithm which uses contourlet transform, SVD, quick response code and Arnold transform for patient authentication. For the medical applications the robustness and security of the watermarking algorithm are very important issues. The proposed algorithm is tested against various attacks and it is concluded that it is robust against JPEG compression attack.

Mohanty et al. [37] proposed a watermarking algorithm which uses Chinese remainder theorem and DCT. The maximum PSNR values for the proposed algorithm is 42 dB. The proposed algorithm is robust against the JPEG compression. Shukla et al. [51] proposed a new data hiding algorithm which combines Advanced Encryption Standard (AES), Least Significant Bit (LSB) substitution and Modified Pixel Value Differencing (MPVD). The data is first compressed using a lossless algorithm. Then after AES encryption for higher security the LSB substitution and MPVD are used for data hiding.

Li et al. [32] presented a new algorithm for maintaining the spatial correlation in the encrypted media using a homomorphic cryptosystem. This is important due to the fact that when the data is encrypted the spatial correlations in the images and video frames are eliminated. This will create significant problems for annotation information embedding in the encrypted media. In the proposed algorithm the LSB layers of smooth blocks are used for adding additional data. Zheng et al. [59] proposed a novel lossless data hiding algorithm based on homomorphic cryptosystem. In contrast with the current data hiding methods which use stream ciphers, homomorphic ciphers are mainly used in data security. In the proposed algorithm the data is embedded using a map between secret bits and modified encrypted media.

The data hiding algorithms suitable for uncompressed images can be further categorized into two major categories: algorithms based on Difference Expansion (DE) such as Integer-to-Integer transformation, Predication-Error Expansion (PEE) and Adaptive Embedding (AE); and algorithms based on Histogram Shifting (HS) [49]. Li et al. [31] proposed a new Prediction-error expansion based watermarking algorithm based on a novel embedding method which uses multiple histograms modification. Li et al. [30] proposed a novel difference-pair-mapping based data hiding algorithm. The proposed data hiding algorithm is a histogram based data hiding algorithm which combines expansion embedding and shifting methods. Furthermore Li et al. [29] proposed a framework for designing histogram shifting data hiding algorithms by deconstructing the algorithm in two stages of shifting and embedding. Coatrieux et al. [11] proposed a new data hiding algorithm which classifies the cover images in order to find the most suitable parts of the image for hiding the data. Semi-fragile watermarking algorithm allow modifications such as compression while keeping the fragility of the watermarking [43]. Li et al. [33] proposed a histogram shifting based algorithm for data hiding in JPEG images. The data is embedded in the high-frequency coefficients in order to ensure a high embedding capacity. In the proposed data hiding algorithm an optimal threshold is used for selection of a Discrete Cosine Transform (DCT) coefficient sub-block. Dragoi et al. [18] proposed an adaptive pixel pairing method to optimize the pairwise watermarking scheme presented by Ou et al. [39].

In another approach the data hiding algorithms are categorized into fragile algorithms and robust algorithms. Shehab et al. [48] proposed a robust watermarking algorithm for

multimodal biometric systems. The proposed algorithm uses the RDWT and biometrics for watermarking. The verification accuracy of the proposed algorithm is 94%. Su et al. [53] proposed a robust and adaptive watermarking algorithm for color images. The proposed algorithm uses a combination of RDWT, ICA, NVF and scrambling techniques. The maximum PSNR values for the proposed algorithm is 53.15 dB. Singh et al. [52] proposed a robust and secure watermarking algorithm which uses the thumbnail feature vector. The proposed algorithm is spectrum based and uses integrity verification. The maximum PSNR values for the watermarked images using the proposed algorithm is 41 dB.

In recent years several new data hiding algorithms have been proposed in both of these categories. Hua et al. [26] presented a new data hiding algorithm based on Random Matching Pursuit (RMP). The security of the proposed algorithm is higher than similar algorithm using random over-complete dictionaries and the order parameter of RMP. Also, using over-complete dictionaries that expand signal dimension, the capacity of the proposed method is better than other data hiding methods. Ding et al. [17] proposed a new data hiding method for halftone images using block conjugate (HQDHBC). They construct Least Mean Square Filters (LMSF), and then use LMSFs to evaluate the quality of halftone images. In the proposed algorithm the images are divided into multiple blocks of  $M \times N$  pixels. If the first  $M \times N - 1$  pixels are conjugate then the last pixel can implement normal halftone method.

Among important applications of data hiding are sensitive data transmission and data authentication. For these applications it is of importance to detect any attempt to tamper with the cover media. The data hiding algorithms can be categorize into robust and fragile algorithms. Robust algorithms are used when the cover image should be able to tolerate the degradation resulting from compression and any other transformation. Robust data hiding can be used for digital watermarking with applications in copyright protection. The reviewed algorithms can hide the data robustly in the cover media with acceptable perceptual quality. However, there are three major problems in these recently proposed algorithms which this work improves upon these problems. The first problem is that currently the performance of the proposed data hiding algorithms and their embedding capacity are dependent on the content of the cover image. The second problem is that the maximum embedding capacity with acceptable perpetual quality can be improved. Finally, the embedding stage in the above mentioned algorithms instead of using the entire cover image, uses variations of search methods for finding special blocks of pixels which are suitable for the embedding process. The proposed algorithm in this work addresses these shortcomings.

### 3 Proposed LVQ based data hiding algorithm

In this section the proposed data hiding algorithm is introduced in details. The proposed data hiding algorithm includes a data embedding phase as well as a data extraction phase. The data embedding phase consists of 6 steps and the data extraction phase includes 5 steps. In order to describe the proposed data hiding algorithm it is necessary to describe lattice vector quantization first. Then the 6 steps of the data embedding phase will be followed in detail.

A finite set of points  $y_1, \dots, y_M$  in an  $n$ -dimensional Euclidean space,  $R^n$ , is called an Euclidean code [13]. An  $n$ -dimensional quantizer is a function  $Q : R^n \rightarrow R^n$  that maps each point  $x \in R^n$  into  $Q(x)$  provided that  $Q(x)$  is the nearest code point. The code points may be selected according to any type of relationship. If the code points are selected from a lattice, then the quantizer would be called a lattice vector quantizer. Lattice vector quantizer reduces the amount of computation for codebook generation since the lattices have regular structures.

An  $n$ -dimensional lattice  $\Lambda$  is considered as a subset of points in the  $n$ -dimensional space that share a common property. The lattice points are usually generated using a generator matrix. The generator matrix of the lattice  $\Lambda$  with the basis vectors  $b_1 = (b_{11}, b_{12}, \dots, b_{1m})$ ,  $b_2 = (b_{21}, b_{22}, \dots, b_{2m})$ , ...,  $b_n = (b_{n1}, b_{n2}, \dots, b_{nm})$  is given as [15]:

$$G = \begin{pmatrix} b_{11} & b_{12} & \cdots & b_{1m} \\ b_{21} & b_{22} & \cdots & b_{2m} \\ \vdots & \vdots & \ddots & \vdots \\ b_{n1} & b_{n2} & \cdots & b_{nm} \end{pmatrix} \quad (1)$$

The Gramm matrix of a lattice  $\Lambda$  is defined as  $\text{Gramm}(\Lambda) = GG'$ , where  $G'$  is the transposed generator matrix  $G$ . If the Gramm matrices of two lattices are proportionate then they are equivalent. The basis vectors of a lattice are linearly independent if and only if the determinant of the Gram matrix is non-zero. There are many ways of choosing a basis and a fundamental parallelopope for a lattice  $\Lambda$ . But the volume of the fundamental region is uniquely determined by  $\Lambda$ , that is  $\text{vol} = \det G = \sqrt{\det \Lambda}$ . If the generator matrix is a square matrix then  $\det \Lambda = (\det G)^2$ . The determinant of a lattice  $\Lambda$  is also equal to the determinant of the Gramm matrix [15],  $\det \Lambda = \det(\text{Gramm}(\Lambda))$ . In an  $n$ -dimensional lattice  $\Lambda$ , the Voronoi region of a lattice point  $\lambda \in \Lambda$  is defined as the union of all non-lattice points within  $\mathbb{R}^n$  that are closer to this particular lattice point than any other lattice point. Thus, the Voronoi region of  $\lambda \in \Lambda$  is defined as [55].

$$V(\lambda) \triangleq \left\{ x \in \mathbb{R}^n : \|x - \lambda\| \leq \|x - \lambda'\|, \forall \lambda' \in \Lambda \right\} \quad (2)$$

As a consequence, all the points within  $V(\lambda)$  must be quantized to  $\lambda$ . The Voronoi region of a sublattice point  $\lambda'$  is the set of all lattice points that are closer to  $\lambda'$  than any other sublattice points. Thus, the Voronoi region of  $\lambda' \in \Lambda'$  is defined as

$$V(\lambda') \triangleq \left\{ \lambda \in \Lambda : \|\lambda - \lambda'\| \leq \|\lambda - \lambda''\|, \forall \lambda'' \in \Lambda' \right\} \quad (3)$$

The index  $N$  is defined as the ratio between the volumes of the sublattice  $\Lambda'$  fundamental parallelopope and the lattice  $\Lambda$  fundamental parallelopope. Thus,  $N$  is calculated by

$$N = \frac{\text{vol}'}{\text{vol}} = \sqrt{\frac{\det \Lambda'}{\det \Lambda}} = \frac{\det G'}{\det G} \quad (4)$$

The index  $N$  determines the number of lattice points within the Voronoi region of the sublattice points. Therefore, the value of  $N$  controls the coarse degree of the sub lattice. A lattice  $A_n$  is a subset of  $(n+1)$ -dimensional points, such that the sum of their coordinates is zero. Therefore, a lattice  $A_n$  can be defined as:

$$A_n = \left\{ (x_0, x_1, \dots, x_n) \in \mathbb{Z}^{n+1} : x_0 + x_1 + \dots + x_n = 0 \right\} \quad (5)$$

The points within the  $A_4$  lattice are generated by

$$G_{A4\_5D} = \begin{pmatrix} -1 & 1 & 0 & 0 & 0 \\ 0 & -1 & 1 & 0 & 0 \\ 0 & 0 & -1 & 1 & 0 \\ 0 & 0 & 0 & -1 & 1 \end{pmatrix} \quad (6)$$

Every  $A_n$  lattice has several  $n$ -dimensional definitions (generator) in addition to the  $(n+1)$ -dimensional definition, Eq. (6). One of the 4-dimensional generators of the  $A_4$  is given as

$$G_{A4\_4D} = \frac{1}{2} \begin{pmatrix} 2 & 0 & 0 & 0 \\ -1 & 1 & 1 & 1 \\ 0 & -2 & 0 & 0 \\ 0 & 1 & -\sigma & -\tau \end{pmatrix} \quad (7)$$

where  $\tau = (1 + \sqrt{5})/2$  and  $\sigma = (1 - \sqrt{5})/2$ . [9] The Gramm matrix of  $G_{A4\_4D}$  is

$$\text{Gramm}(A_{A4\_4D}) = G_{A4\_4D} G_{A4\_4D}' = \frac{1}{2} \begin{pmatrix} 2 & -1 & 0 & 0 \\ -1 & 2 & -1 & 0 \\ 0 & -1 & 2 & -1 \\ 0 & 0 & -1 & 2 \end{pmatrix} = \frac{1}{2} (\text{Gramm}(A_{A4\_5D})) \quad (8)$$

Equation (8) indicates that the lattice generated by Eq. (6) is similar to the lattice generated by Eq. (7) because the Gramm matrices are proportionate. Therefore, this definition enables the user to employ the quaternion algebra, based on the inclusion of a root system of type  $A_4$  within a type of  $H_4$  [9]. The reason to choose  $G_{A4\_4D}$  among different descriptions of  $A_4$  is that the basis vectors of  $G_{A4\_4D}$  are members of the icosian ring  $\mathbf{I}$  [9]. The icosian group is a multiplicative group of order 120 consisting of all even permutations of the quaternions in the form of [15]:

$$\frac{1}{2}(\pm 2, 0, 0, 0) \text{ or } \frac{1}{2}(\pm 1, \pm 1, \pm 1, \pm 1) \text{ or } \frac{1}{2}(0, \pm 1, \pm \sigma, \pm \tau) \quad (9)$$

where  $(\alpha, \beta, \gamma, \delta)$  are coordinates of a quaternion  $q = \alpha + \beta i + \gamma j + \delta k$ . The coordinates belong to the golden quadratic field. The icosian ring  $I$  is the set of all finite sums  $q_1 + q_2 + \dots + q_n$ , where each  $q_i$  is a member of the icosian group. An important property of the icosian group is that for any icosian  $\mathbf{p}$  and  $\alpha \in \mathbb{Q}$ , the mapping  $x \rightarrow \alpha \mathbf{p} x \tilde{\mathbf{p}}$  is an orientation preserving transformation from icosian group to icosian group. Thus, there are 120 transformations that can generate 120 similar sublattices of  $A_4$ , which are in one-to-one relation with the lattice generator defined in Eq. 11

$$\mathbf{L}_i = (\mathbf{p}_i * G_{A4\_4D}) * \tilde{\mathbf{p}}_i, \quad i = 1 \dots 120 \quad (10)$$

where  $*$  is a quaternion product between  $\mathbf{p}_i$  and every row of  $G_{A4\_4D}$ , and  $\tilde{\mathbf{p}}_i$  is the twist-mapped version of  $\mathbf{p}_i$ . Thus, all similar sublattices of  $A_4$  are images of  $G_{A4\_4D}$  under orientation preserving mappings of Eq. (10) [9]. In fact, the icosian ring consists of 60 different elements of the form  $\pm \mathbf{p}$ . As a consequence, there are 60 pairs of generator matrices available with the same Gramm matrices.

Fast quantizing algorithms are a family of LVQ algorithms presented in [14] for different root lattices. The quantization using  $A_n$  lattice points is a projection from  $n$ -dimensional space onto  $\sum_{i=1}^{n+1} x_i = 0, x_i \in \mathbb{Z}$  hyper plane. The fast quantizing algorithm first projects the  $n$ -dimensional input vector onto a  $(n+1)$ -dimensional vector on  $\sum_{i=1}^{n+1} x_i = 0, x_i \in \mathbb{R}$  hyper-plane using a transformation matrix [14]. Then, using a manipulation the projected point is mapped onto a lattice point. As an example consider the  $A_4$  lattice, the input must be mapped into a 5 dimensional hyper planes. The transformation matrix which is necessary for the LVQ is calculated using the relation between

5-dimensional generator Eq. (6) and the 4-dimensional generator Eq. (7) [4]. The relation is as follows [1]:

$$T = (G_{A4\_4D})^{-1} \times G_{A4\_5D} = \frac{1}{\tau-\sigma} \begin{pmatrix} \sigma-\tau & \tau-\sigma & 0 & 0 & 0 \\ 0 & 0 & \tau-\sigma & \sigma-\tau & 0 \\ -\tau & -\tau & -\sigma & -\sigma & 2 \\ \sigma & \sigma & \tau & \tau & -2 \end{pmatrix} \quad (11)$$

In the proposed watermarking algorithm a sublattice of  $A_4$  with index  $N=4$  is used.

### 3.1 Data embedding phase

The embedding algorithm is implemented in discrete wavelet transform domain. One of the major problems in image watermarking based on IIDWT is overflow and underflow [49]. This problem arises when pixels with values ranged between [0, 16] or [239, 255] are transformed into frequency domain and after embedding stage transformed back into the spatial domain. Depending on the embedded data, their values may be outside the [0, 255] range. In order to avoid the problem of overflow or underflow, a histogram manipulation is performed on the cover image. The grey-scale levels of pixels at the upper and lower bounds of the histogram shrunk towards the average by 16 greyscale values. Consequently, the pixels with greyscale levels of [0, 16] and [239, 255] will no longer be found in the image. This action will prevent the problem of overflow and underflow in the watermarking stage. The removal of these greyscale levels has limited adverse effect on the quality of the image in terms of PSNR.

It is possible to apply the algorithm to a part of the cover image rather than the whole image based on the amount of the TBE data (the sensitive data). The  $512 \times 512$  cover image divided into  $64 \times 64$  blocks which will result is 64 blocks. The placement and the size of the selected blocks can vary based on sensitive data size.

Embedding data in the image result in significant degradation in perceptual quality of the image from human perspective. The human eye perceives the image with hidden data as containing a spatial distortion which is undesirable as the watermarking algorithm's outcome. To avoid this outcome, we should remove the spatial relation between pixels in the image by wavelet transform and embed the data in the frequency domain. The effect of the distortion in the resulted image is no longer perceivable with human eye. The input cover image is transformed into frequency domain using lifting Integer-to-Integer discrete wavelet transform (IIDWT). The wavelet transform is introduced in Mallat [36] as a part of multi-resolution theory. The second generation of wavelet transforms are wavelets with lifting schemes presented in [54]. In this new generation of wavelet transforms the process of constructing the wavelets and performing the discrete wavelet transforms are performed concurrently. The lifted Integer-to-Integer Cohen-Daubechies-Feauveau CDF (2, 2) wavelet is used as the DWT.

If any block of  $64 \times 64$  pixels is transformed to frequency domain using IIDWT, the approximation, V, D and H sub-bands with  $32 \times 32$  size are calculated. The TBE data should not be embedded in the approximation sub-band since it will result in significant visual degradation in the cover image. Next the DWT coefficients in V, D and H sub-bands are reshaped into 2D matrix having four columns and variable rows. Every row is used to embed six bits of data, two bits sensitive data element (which must be kept hidden) and four bits for LVQ error correction.

As mentioned above two least significant bits are reserved for the sensitive data and four most significant bits are reserved for the quantization error indices data. Thus, it is possible to embed two bits of sensitive data using four grey scale pixel values. There are  $32 \times 32 = 1024$

DWT coefficients in every subband, therefore it is possible to embed 512 bits in each subband and 1536 in every  $64 \times 64$  block. Based on the amount of sensitive data, several blocks of the cover image are selected, that is one block per 1536 bits.

The selected number of blocks of the image are first transformed into DWT coefficients by IIDWT and then these coefficients are lattice vector quantized using the  $A_4$  sub-lattice with  $N=4$ . There are sixty four  $Z_4$  lattice points within the Voronoi of every  $A_4$  sub-lattice point. The embedding can be implemented using these sixty four  $Z_4$  lattice points. Based on the value of the sensitive data the  $A_4$  sub-lattice point is mapped on one of these sixty four  $Z_4$  lattice points.

In fact, one embedding key is randomly generated by the user. This embedding key is used for creation of a mapping table which in turn determines which  $Z_4$  lattice point is selected for the mapping process. Since it is not possible to demonstrate this concept visually as lattice vectors in this stage are of the dimension of five, we demonstrate this concept in a two dimensional abstraction using  $A_2$  and  $Z_2$  lattice points Table 1.

Let the selected block have  $R_{row} \times C_{col}$  pixels. The output of the IIDWT are three  $R_{row}/2 \times C_{col}/2$  subbands. The subband coefficients are vectorized and lattice vector quantized on sub- $A_2$ -lattice with  $N=1$ , which are shown by red parallelograms in Fig. 1. The points of  $Z_2$  lattice are shown with blue squares. According to the sensitive data bits, the sub- $A_2$ -lattice is mapped one of these  $Z_2$  points.

However, it is observed that there are  $Z_2$  lattice points in equal distance from more than one  $A_2$ . If these  $Z_2$  lattice points are used for embedding, there will be ambiguity in data extraction since there would be two alternatives for the location of the  $Z_2$  lattice points. To prevent this kind of ambiguity we have to use a clean sub-lattice of  $A_2$ . The sublattices of  $A_2$  are clean, if and only if,  $\alpha$  and  $\beta$  are relatively primes. It follows that  $A_2$  has a clean similar sublattice of index  $N$  if and only if  $N$  is a product of primes congruent to 1 (mod 6) [12]. The first clean sub-lattice of  $A_2$  is with index  $N=7$ .

In Fig. 2 sub- $A_2$  lattice points with red parallelograms, the Voronoi of sub- $A_2$  lattice points with  $N=7$  are shown with blue hexagons and  $Z_2$  lattice points are shown with blue squares. According to inherent symmetries of  $A_2$  sub-lattices, it is possible to count the number of  $Z_2$  lattice points inside these six Voronoi and generalize the results to the entire  $A_2$  sub-lattice with  $N=7$ . There are either four or six  $Z_2$  lattice points inside the Voronoi of  $A_2$  sub-lattice with  $N=7$ .

As shown in the Fig. 2 there are several  $Z_2$  lattice points inside the Voronoi of each  $A_2$  lattice point. If any of the sub- $A_2$  lattice points are mapped to any  $Z_2$  lattice points within its corresponding Voronoi, it is possible to remap it back to their original  $A_2$  lattice point by a lattice vector quantization. The next step is the decision about the  $Z_2$  lattice point which is selected for mapping. Depending on the given sensitive data sub- $A_2$  lattice point is mapped on one of the  $Z_2$  lattice points. There are four possible mapping positions. Table 2 demonstrates a hypothetical mapping for the embedding process for the sub-lattice of  $A_2$  ( $N=7$ ).

**Table 1** shows the number of  $Z_2$  lattice points inside the Voronoi of sub-lattice point around the origin

$A_2$ sub-lattice with $N=7$	Number of $Z_2$ lattice points	$A_2$ sub-lattice with $N=7$	Number of $Z_2$ lattice points
(0, 0)	6	( $-2, -\sqrt{3}$ )	6
(0.5, $-\sqrt{3}$ )	4	( $2.5, -0.5\sqrt{3}$ )	6
( $-0.5, 1.5\sqrt{3}$ )	4	( $-2.5, 0.5\sqrt{3}$ )	6
( $2, \sqrt{3}$ )	6		

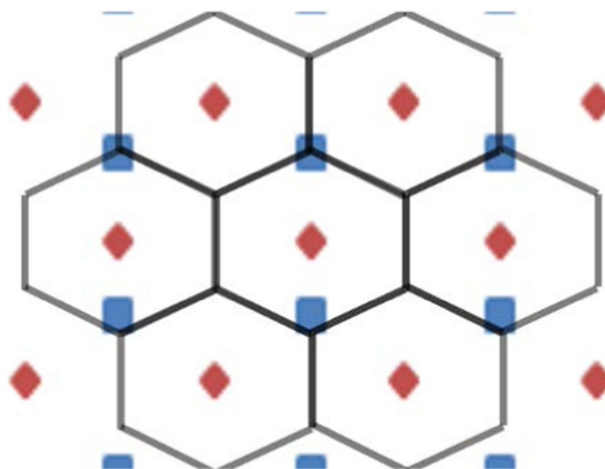


**Fig. 1** Lattice  $Z_2$  and sub-lattice of  $A_2$  with  $N=1$  as well as their Voronoi are shown. The  $Z_2$  lattice points are shown with blue squares. It is observed that there are  $Z_2$  lattice points that are with equal distance to several  $A_2$  sub-lattice points

In the proposed data hiding algorithm sub- $A_4$  lattice with  $N=4$  and  $Z_4$  lattice points are used. The TBE data will be considered to determine which of the four positions will be selected for the mapping. According to an injective mapping table the position of each TBE data will be selected. Then each of these quadruple DWT coefficients are mapped to a sub-lattice of  $A_4$  with the index of  $N=4$ . The embedding process for the sub-lattice of  $A_4$  with the index of  $N=4$  is partly depicted in Table 3.

In general lattices have inherent symmetries which we can use for partitioning the space. Every relation which is correct for the origin of the lattice and the corresponding Voronoi is applicable to the original lattice and all the lattice points. In our case if we consider the origin of the lattice and all the  $A_4$  sub-lattice points around the origin, and calculate the distance

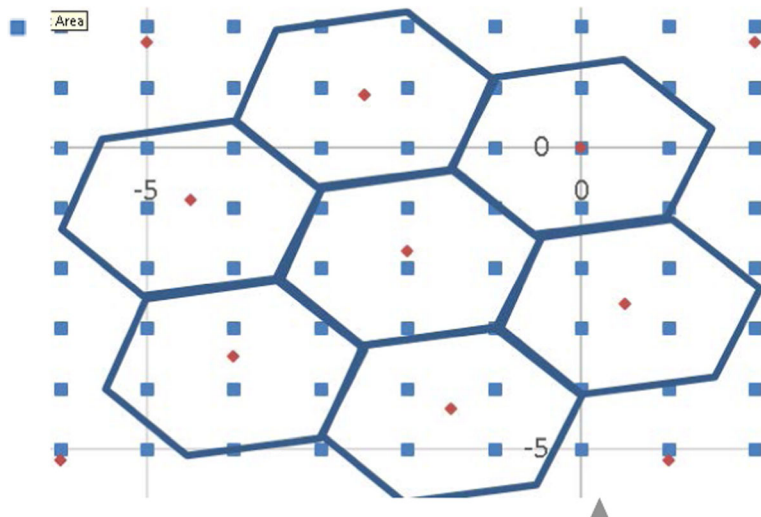


**Fig. 2** Lattice  $Z_2$  and sub-lattice of  $A_2$  with  $N=7$  as well as their Voronoi are shown. It is observed that there are either four or six  $Z_2$  lattice points inside the Voronoi of  $A_2$  sub-lattice with index  $N=7$

**Table 2** A hypothetical mapping table for the embedding process for the sub-lattice of  $A_2$  ( $N=7$ )

TBE bits	Action
00	Map the quantized $A_2$ sub-lattice point to nearest $Z_2$ which has greater $x$ coordinate and greater $y$ coordinate
01	Map the quantized $A_2$ sub-lattice point to nearest $Z_2$ which has greater $x$ coordinate and smaller $y$ coordinate
10	Map the quantized $A_2$ sub-lattice point to nearest $Z_2$ which has smaller $x$ coordinate and greater $y$ coordinate
11	Map the quantized $A_2$ sub-lattice point to nearest $Z_2$ which has smaller $x$ coordinate and smaller $y$ coordinate

between all the  $Z_4$  lattice points to these sub-lattice points it will become apparent that there are only eighty one  $Z_4$  lattice points in the Voronoi of the origin as well as any other  $A_4$  sub-lattice point. As the encoding process uses the binary data, sixty four closest  $Z_4$  lattice points are selected for the encoding bins. Thus, there are sixty four possible mapping positions. The TBE data will be considered to determine which of these sixty four positions will be selected for mapping. In this stage the TBE data and any injective mapping table will determine which of the sixty four positions are selected.

In order to be able to compare the proposed data hiding algorithm with other data hiding algorithms which increase, the size of the smallest blocks in this paper is selected to be  $64 \times 64$  pixels which results 1536-bit steps. The maximum embedding capacity for the entire 64 blocks would be 98,304 bits, which is equal to 0.375 bits per grey-scale pixel. For an RGB image with similar size the maximum embedding capacity would be 288 Kbits or 1.125 bits per RGB pixel.

There are two types distortions introduced during the proposed data hiding algorithm. The first is due to the lattice vector quantization error and the second is due to the embedding. The later distortions is reversible but the former is not reversible. In order to compensate the former distortions, the difference between the quantized coefficients and the original coefficients are calculated and clustered using the K-Means algorithm into sixteen clusters. The index of the centroids of the clustered are inserted into the four significant bits of the TBE. This 256-bit table of the cluster centroid values is saved in the H-sub band of the first  $64 \times 64$  block.

Finally, the embedded coefficients are reshaped to  $32 \times 32$  block subband blocks, then transformed back to the spatial domain using inverse CDF (2, 2) IIDWT and written on the disk.

### 3.2 Data extraction phase

The extraction phase is started with reshaping the cover image with embedded data into 64 blocks of  $64 \times 64$  pixels. Then, every block is transformed into the frequency domain using lifted CDF (2, 2) IIDWT. The calculated DWT coefficients are vectorized into a matrix with four columns. Finally the rows of the calculated matrix is lattice vector quantized. The

**Table 3** A fraction of the mapping used for the embedding process for the sub-lattice of  $A_4$  ( $N=4$ )

TBE bits	Required translation						
000000	[0, 0, 0, 0]	000100	[-1,-1,0,1]	000010	[-1,-1,0,-1]	000110	[-1,0,1,-1]
000001	[-1,-1,-1,0]	000101	[-1,-1,1,0]	000011	[-1,-1,0,0]	000111	[-1,0,-1,0]

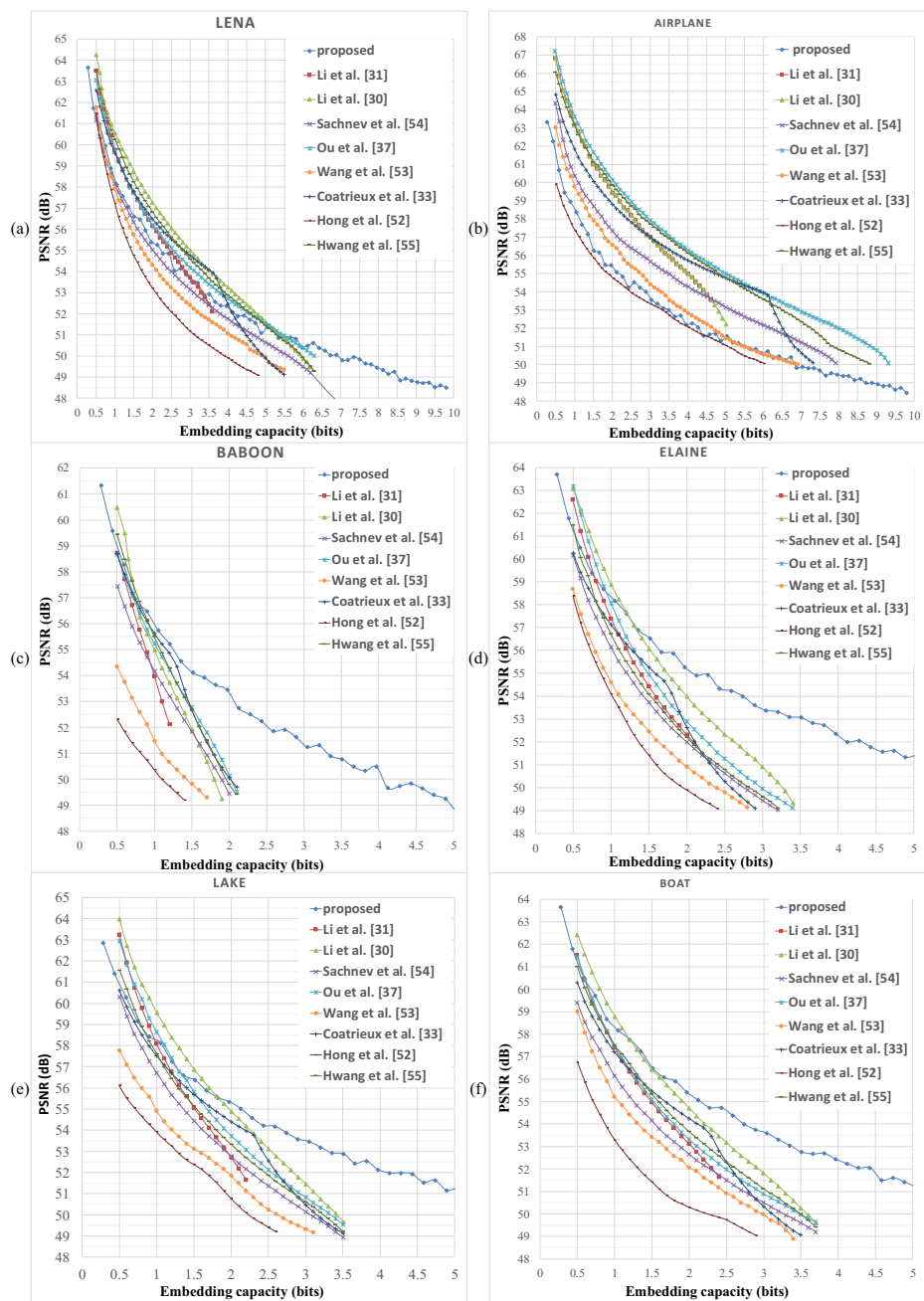


**Fig. 3** Performance comparison of the proposed data hiding algorithm for **a** Lena, **b** Airplane, **c** Baboon, **d** Elaine, **e** Lake and **f** Boat

**Table 4** A fraction of the mapping used for the embedding process of for the sub-lattice of  $A_4$  ( $N = 4$ )

Calculated translation	Extracted data bits	Calculated translation	Extracted data bits
[0,0,0, 0]	000000	[1, 1, 0, 1]	000100
[1,1,1,0]	000001	[1,1,-1,0]	000101
[1,1,0,1]	000010	[1,0, 1, 1]	000110
[1, 1, 0, 0]	000011	[1,0, 1, 0]	000111

difference between the original matrix and the quantized matrix is found. The result of the subtraction is a translation vector, which can be used to determine the corresponding mapping which had already been applied in the embedding phase. Since this mapping is determined based on the TBE data it would be possible to reverse map the translation vector to the exact embedded data. A fraction of the mapping used for the embedding process of for the sub-lattice of  $A_4$  ( $N = 4$ ) is depicted in Table 4.

The extracted data values are six bits. Two bits are sensitive data and four bits are error compensation indices. In order to compensate the distortions introduced by the quantization error, the four most significant bits of the extracted six-bit data is used to find the corresponding cluster head in the cluster head table.

## 4 Experimental results

In this section we evaluate the performance of the proposed data hiding algorithm and compare the experimental results with several recent algorithms proposed in the literature. The proposed method is applicable to any image with any size, grey-scale or RGB. To be able to compare the performance of the proposed data hiding algorithm, we used six standard grey-scale images

**Table 5** Embedding capacity comparison for the same PSNR = 55 dB measured in Kbits

Image	[24]	[56]	[47]	[27]	[30]	[39]	[11]	[31]	proposed
Lena	14.00	17.00	20.00	28.00	23.90	25.00	28.00	30.90	21.5
Baboon	1.00	4.00	8.00	9.90	7.90	9.90	11.00	10.90	20.75
Airplane	18.10	27.10	34.10	47.20	39.20	49.10	47.10	39.10	20.75
Elaine	7.90	8.90	11.20	12.90	12.90	13.90	14.90	16.90	20
Lake	6.90	9.90	13.00	14.90	14.90	15.90	17.00	18.90	20.75
Boat	7.00	10.00	12.00	15.00	14.90	15.00	16.00	19.00	20.75
Average	9.15	12.82	16.38	21.32	18.95	21.47	22.33	22.62	20.75

**Table 6** Performance comparison with other existing algorithms with 175,000 embedded bits

Image	[24]	[56]	[47]	[27]	[30]	[39]	[11]	[31]	proposed
Lena	53.78	55	55.6	57.5	56.9	56.9	57.2	58	56.2
Baboon	—	49.2	50.7	51.2	—	51.6	51.2	50.4	53.75
Airplane	55.2	57.4	58	60.5	60.2	60.8	59.4	60.2	55.8
Elaine	50.5	51.6	52.8	53.1	53.3	53.8	54.4	55	55.87
Lake	51.7	52.5	53.6	54.2	53.9	54.7	55	55.7	55.8
Boat	50.7	52.7	53.3	54.4	54	54.2	54.8	55.6	56
Average	52.38	53.07	54.00	55.15	55.66	55.33	55.33	55.82	55.57

namely, Lena, Baboon, Airplane, Elaine, Lake and Boat for our experiments. The experimental results are compared with algorithms proposed in [11, 24, 27, 30, 31, 39, 47, 56].

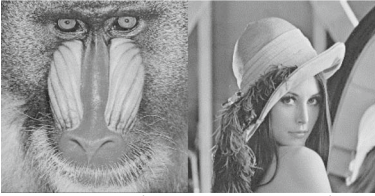
Prediction Error Expansion based method outperforms these seven algorithms. All the images used for experimental results are of the size  $512 \times 512$  and downloaded from the USC-SIPI database [57]. Figure 3 demonstrates the performance comparison of the proposed data hiding algorithm with eight algorithms mentioned above. In Fig. 3 we start with the low TBE data amount and increased the TBE data by 1536 bits in every step.

The proposed data hiding algorithm performs uniformly well across all the reference images compare to the PEE based reference algorithms. The reference algorithms show better results on Baboon, Elaine, Lake and Boat images but are unable to show the same performance on more complex reference images such as Lena and Airplane. We believe that the advantage of the proposed data hiding algorithm is the result of independence from context of the cover image. The LVQ based embedding in contrast to histogram based algorithms is independent of the numerical distribution of the pixel values in the image.

Based on Fig. 3 the proposed data hiding algorithm has several advantages. The first advantage is that the performance of watermarking algorithms and embedding capacity in other algorithms are dependent on the content of the cover image, but the proposed data hiding algorithm performs with high performance across most of the cover images. For Example as seen in [31], the embedding capacity of those algorithms applied to the cover image of Baboon image is significantly less than the Lena.

For Baboon, the maximum embedding capacity with acceptable PSNR, above 50 dB, is 21 Kbits, whereas for Baboon we can achieve 38 Kbits with the same PSNR. The second advantage is that in the reference algorithms the maximum embedding capacity for the cover image of Lena for PSNR values above 50 dB is 61.4 Kbits, whereas the proposed data hiding algorithm is capable of embedding 67 Kbits in Lena with the same PSNR value.

Table 5 shows the embedding capacity of the proposed data hiding algorithm compared to the same reference algorithms in Fig. 3 for the same PSNR = 55 dB measured in Kbits. This table shows that the proposed data hiding algorithm outperforms Li et al. [31] when applied to images of Baboon, Elaine, Lake, and Boat.

Embedde d data (bits)	Grey-scale images		Embedde d data (bits)	Grey-scale images	
	Baboon	Lena		Baboon	Lena
18176			50432		
	PSNR = 53.63 dB	PSNR = 53.80 dB		PSNR = 48.80 dB	PSNR = 49.03 dB
35072			98048		
	PSNR = 50.78 dB	PSNR = 50.81 dB		PSNR = 45.93 dB	PSNR = 48.51 dB

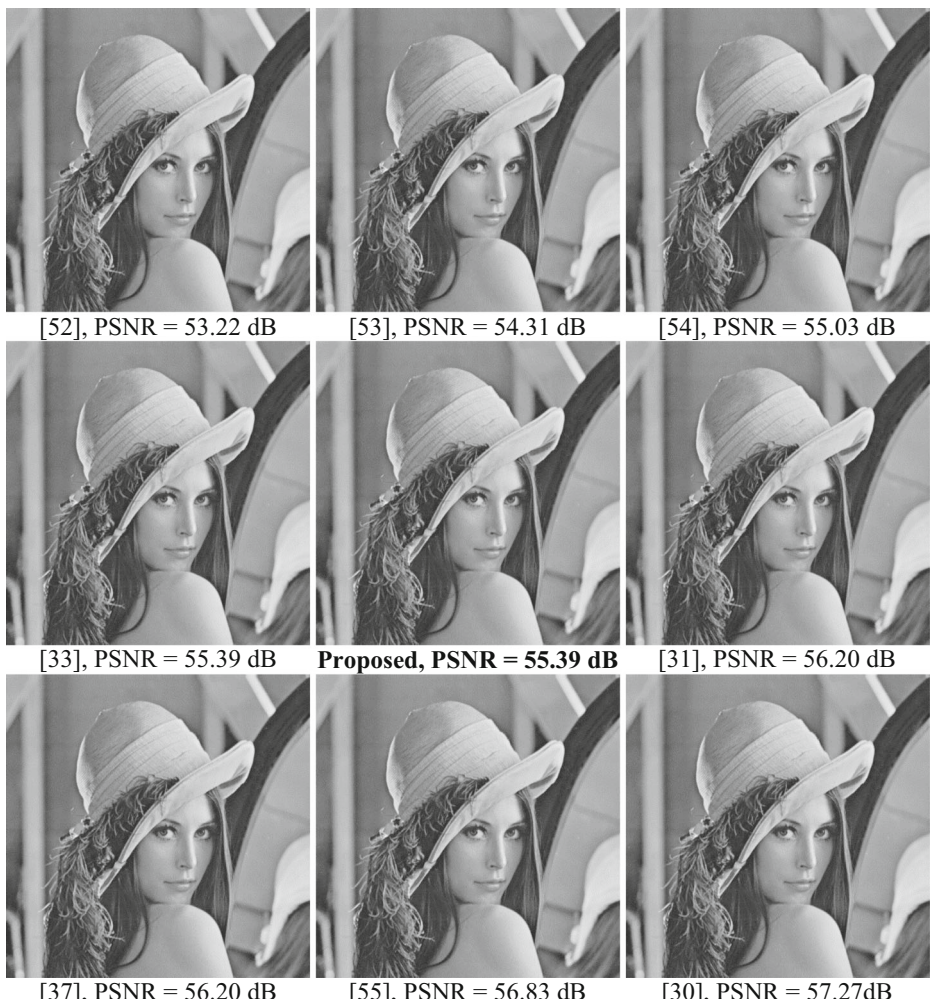
**Fig. 4** Performance comparison of the proposed data hiding algorithm for **a** Lena **b** Baboon

Table 6 demonstrates the performance comparison of the proposed data hiding algorithm for Lena, Baboon, Airplane, Elaine, Lake and Boat for 175,000 embedded bits with the same reference algorithm in Fig. 3. As shown in Table 6 the proposed data hiding algorithm outperforms Li et al. [31] when applied to images of Baboon, Elaine, Lake, and Boat.

Figure 4 demonstrates the quality of the cover images with embedded data with different embedded data sizes.

As shown in Fig. 4 the quality of the cover images in grey scale do not show any perceptual degradation with increasing the amount of TBE data. Figure 4 shows that the cover images after embedding 98,048 bits for grey scale retaining the PSNR values of above 48 dB.

In order to compare the results of the proposed algorithm with the comparative methods visually, the results of embedding performance for Lena and Boat cover images with the embedding data of 20 Kbits are presented in Figs. 5 and 6.



**Fig. 5** Performance comparison of the proposed data hiding algorithm with other proposed algorithms in Lena with the embedding data of 20 Kbits

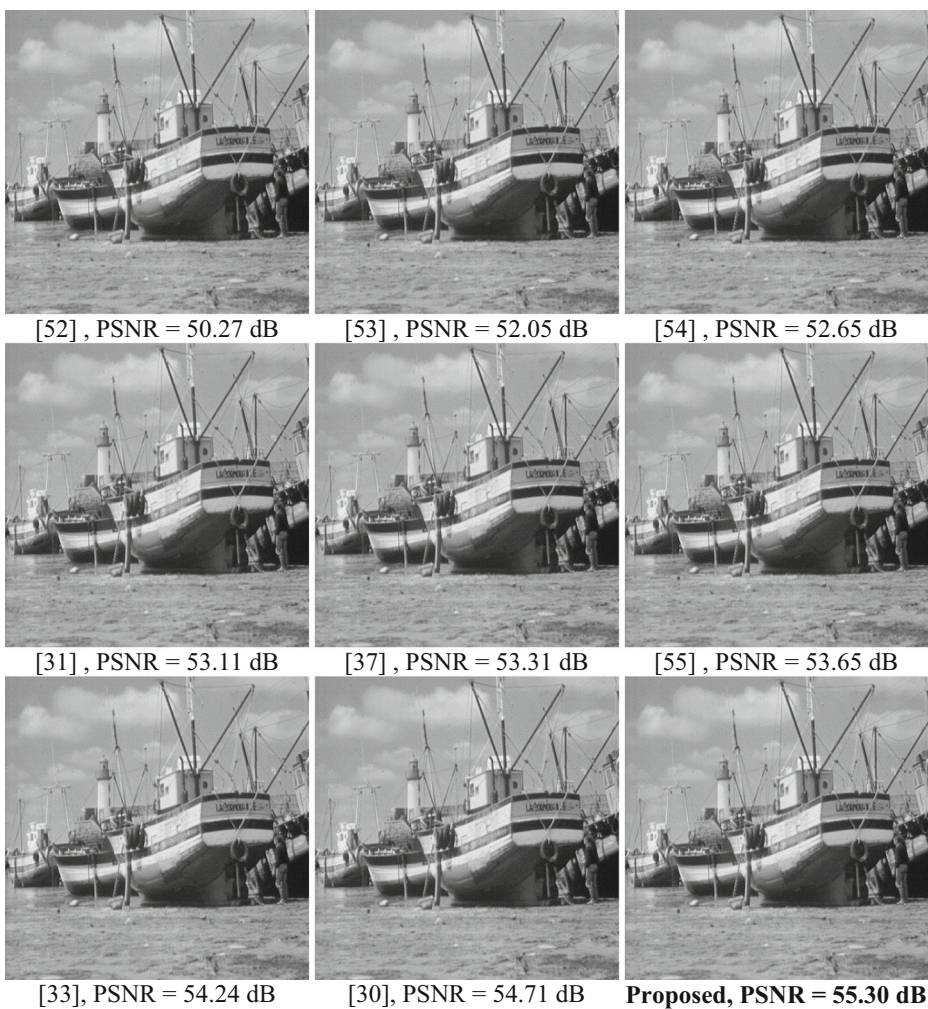


**Fig. 6** Performance comparison of the proposed data hiding algorithm with other proposed algorithms in Boat with the embedding data of 20 Kbits

#### 4.1 Future works

The visual saliency is able to control the strength of watermark embedding. This capability can be used to improve the imperceptibility and robustness of watermarking. An interesting topic for further expanding the proposed data hiding algorithm is using image saliency [19]. There are two avenues for improving the data hiding algorithms using image saliency. The Saliency map in an image provides the areas of an image which are rich in information. These areas can be used for data hiding in order to resist various attacks and corruptions and therefore can increase the robustness of the proposed algorithm. Detecting salient objects [20, 35] and embedding data in those regions can improve imperceptibility of the data hiding algorithm. The second pathway is to increase the capacity of the proposed embedding method can be improved by embedding data in the D domain of the RGB-D [20] images.

## 5 Conclusion

In this paper a novel watermarking algorithm based on LVQ is proposed. The proposed data hiding algorithm is a fragile data hiding algorithm which is able to embed the data inside the entire image. The algorithm is based IIDWT and LVQ. The proposed data hiding algorithm embeds the data using re-quantization of already  $A_4$  sub-lattice vector quantized into  $Z_4$  lattice points according to the TBE and a mapping table. The simulation results show that the proposed algorithm is capable of performing significantly better than the recently proposed algorithms when the amount of TBE data in the images is high. The proposed data hiding algorithm can embed more data in the same cover images compared to other watermarking algorithms while keeping the quality of the cover image at an acceptable level of PSNR higher than 50 dB. For embedding capacities higher than 20 Kbits the proposed data hiding algorithm demonstrates higher perceptual quality in terms of PSNR. In addition the proposed data hiding algorithm can produce high embedding capacity with acceptable PSNR in a wide range of the cover images.

## References

1. Akhtarkavan E (2012) Multiple-description lattice vector quantization for image and video coding based on coinciding similar sublattices of  $A_n$ , in School of Electrical and Electronics. Universiti Sains Malaysia: <http://ee.eng.usm.my/eeacad/fadzli/abstract/Phd-06-12-Abstract.pdf>, p. 169.
2. Akhtarkavan E, Majidi B, Manzuri MT (2019) Secure communication and archiving of low altitude remote sensing data using high capacity fragile data hiding. *Multimed Tools Appl* 78(8):10325–10351
3. Akhtarkavan E, Salleh MFM (2010) Multiple description lattice vector quantization using multiple  $A_4$  quantizers. *IEICE Electronics Express* 7(17):1233–1239
4. Akhtarkavan E, Salleh MFM (2010) Multiple description lattice vector quantization using multiple  $A_4$  quantizers. *IEICE Electronics Express* 7(17):1233–1239
5. Akhtarkavan E, Salleh MFM (2011) Multiple descriptions coding for H.264/AVC using coinciding  $A_2$  lattice vector quantizer. in 2011 IEEE International Conference on Signal and Image Processing Applications (ICSIPA)
6. Akhtarkavan E, Salleh MFM (2012) Multiple descriptions coinciding lattice vector Quantizer for wavelet image coding. *IEEE Trans Image Process* 21(2):653–661
7. Akhtarkavan E, Salleh M (2012) Multiple Descriptions Coinciding Lattice Vector Quantizer for H. 264/ AVC and Motion JPEG2000, in Advanced Video Coding for Next-Generation Multimedia Services, Y.-S. Ho, Editor, Electronics and Telecommunications Research Institute IntechOpen: South Korea
8. Akhtarkavan E, Salleh M, Sidek O (2013) Multiple descriptions video coding using coinciding lattice vector Quantizer for H. 264/AVC and motion JPEG2000. *World Appl Sci J* 21(2):157–169
9. Baake M, Heuer M, Moody RV (2008) Similar sublattices of the root lattice  $A_4$ . *Journal of Algebra* 320(4): 1391–1408
10. Chang I-C et al (2015) High capacity reversible data hiding scheme based on residual histogram shifting for block truncation coding. *Signal Process* 108:376–388
11. Coatrieux G et al (2013) Reversible watermarking based on invariant image classification and dynamic histogram shifting. *IEEE Transactions on Information Forensics and Security* 8(1):111–120
12. Conway JH, Rains EM, Sloane NJA (1999) On the existence of similar sublattices. *Can J Math* 51:1300–1306
13. Conway JH, Sloane NJA (1982) Voronoi regions of lattices, second moments of polytopes and quantization. *IEEE Trans on Information Theory* 28(2):211–226
14. Conway JH, Sloane NJA (1982) Fast quantizing and decoding and algorithms for lattice quantizers and codes. *IEEE Trans on Information Theory* 28(2):227–232
15. Conway JH, Sloane NJA (1998) *Sphere Packings, Lattices and Groups*, 3rd edn. Springer-Verlag, New York
16. Das C et al (2014) A novel blind robust image watermarking in DCT domain using inter-block coefficient correlation. *AEU-International Journal of Electronics and Communications* 68(3):244–253

17. Ding H et al (2018) High Quality Data Hiding in Halftone Image Based on Block Conjugate. *Chin J Electron* **27**(1):150–158
18. Dragoi IC, Coltuc D (2016) Adaptive pairing reversible watermarking. *IEEE Trans Image Process* **25**(5): 2420–2422
19. Fan D-P et al (2018) Salient objects in clutter: Bringing salient object detection to the foreground. in Proceedings of the European Conference on Computer Vision (ECCV)
20. Fan, D.-P., et al., Rethinking rgb-d salient object detection: models, datasets, and large-scale benchmarks. 2019.
21. Gersho A, Gray RM (2003) Vector quantization and signal compression, 9th edn. Kluwer Academic Publishers, Amsterdam
22. Goyal VK, Kelner JA, Kovacevic J (2002) Multiple description vector quantization with a coarse lattice. *IEEE Trans Inf Theory* **48**(3):781–788
23. Gunjal BL, Mali SN (2015) MEO based secured, robust, high capacity and perceptual quality image watermarking in DWT-SVD domain. *SpringerPlus* **4**(1):126
24. Hong W, Chen T-S, Shiu C-W (2009) Reversible data hiding for high quality images using modification of prediction errors. *J Syst Softw* **82**(11):1833–1842
25. Hossain MS, Muhammad G (2016) Cloud-assisted industrial internet of things (iiot)—enabled framework for health monitoring. *Comput Netw* **101**:192–202
26. Hua G et al (2019) Random matching pursuit for image watermarking. *IEEE Transactions on Circuits and Systems for Video Technology* **29**(3):625–639
27. Hwang HJ et al (2010) Reversible watermarking method using optimal histogram pair shifting based on prediction and sorting. *KSII Transactions on Internet and Information Systems (TIIIS)* **4**(4):655–670
28. Kalra GS, Talwar R, Sadawarti H (2015) Adaptive digital image watermarking for color images in frequency domain. *Multimed Tools Appl* **74**(17):6849–6869
29. Li X, Li B, Yang B, Zeng T (2013) General framework to histogram-shifting-based reversible data hiding. *IEEE Trans Image Process* **22**(6):2181–2191
30. Li X et al (2013) A novel reversible data hiding scheme based on two-dimensional difference-histogram modification. *IEEE Transactions on Information Forensics and Security* **8**(7):1091–1100
31. Li X et al (2015) Efficient reversible data hiding based on multiple histograms modification. *IEEE Transactions on Information Forensics and Security* **10**(9):2016–2027
32. Li M et al (2019) Fidelity preserved data hiding in encrypted highly autocorrelated data based on homomorphism and compressive sensing. *IEEE Access* **7**:69808–69825
33. Li Y et al (2019) A high-imperceptibility and histogram-shifting data hiding scheme for JPEG images. *IEEE Access* **7**:73573–73582
34. Linde Y, Buzo A, Gray R (1980) An algorithm for vector quantizer design. *IEEE Trans on Communications* **28**(1):84–95
35. Liu Y et al (2019) DNA: Deeply-supervised Nonlinear Aggregation for Salient Object Detection
36. Mallat SG (1989) A theory for multiresolution signal decomposition: the wavelet representation. *IEEE Trans on Pattern Analysis and Machine Intelligence* **11**(7):674–693
37. Mohanty SP et al (2017) Everything you want to know about watermarking: from paper Marks to hardware protection: from paper marks to hardware protection. *IEEE Consumer Electronics Magazine* **6**(3):83–91
38. Nguyen TV, Patra JC (2008) A simple ICA-based digital image watermarking scheme. *Digital Signal Processing* **18**(5):762–776
39. Ou B, Li X, Zhao Y, Ni R, Shi YQ (2013) Pairwise prediction-error expansion for efficient reversible data hiding. *IEEE Trans Image Process* **22**(12):5010–5021
40. Pan Z, Wang L (2018) Novel reversible data hiding scheme for two-stage VQ compressed images based on search-order coding. *J Vis Commun Image Represent* **50**(50):186–198
41. Patra JC, Karthik A, Bornand C (2010) A novel CRT-based watermarking technique for authentication of multimedia contents. *Digital Signal Processing* **20**(2):442–453
42. Patra JC, Phua JE, Bornand C (2010) A novel DCT domain CRT-based watermarking scheme for image authentication surviving JPEG compression. *Digital Signal Processing* **20**(6):1597–1611
43. Piper A, Safavi-Naini R (2013) Scalable fragile watermarking for image authentication. *IET Inf Secur* **7**(4): 300–311
44. Qin C, Hu Y-C (2016) Reversible data hiding in VQ index table with lossless coding and adaptive switching mechanism. *Signal Process* **129**:48–55
45. Rahmani P, Dastghaibyfard G (2018) An efficient histogram-based index mapping mechanism for reversible data hiding in VQ-compressed images. *Inf Sci* **435**(435):224–239
46. Rahmani P, Dastghaibyfard G (2018) Two reversible data hiding schemes for VQ-compressed images based on index coding. *IET Image Process* **12**(7):1195–1203

47. Sachnev V et al (2009) Reversible watermarking algorithm using sorting and prediction. *IEEE Transactions on Circuits and Systems for Video Technology* 19(7):989–999
48. Shehab A et al (2018) Secure and robust fragile watermarking scheme for medical images. *IEEE Access* 6: 10269–10278
49. Shi YQ et al (2016) Reversible data hiding: advances in the past two decades. *IEEE Access* 4:3210–3237
50. Shirafkan MH, Akhtarkavan E, Vahidi J (2015) A image steganography scheme based on discrete wavelet transform using lattice vector quantization and reed-solomon encoding. in 2015 2nd International Conference on Knowledge-Based Engineering and Innovation (KBEI)
51. Shukla AK et al (2018) A secure and high-capacity data-hiding method using compression, encryption and optimized pixel value differencing. *IEEE Access* 6:51130–51139
52. Singh AK, et al (2016) Digital image watermarking: techniques and emerging applications, in *Handbook of research on modern cryptographic solutions for computer and cyber security*. IGI Global. p. 246–272
53. Su Q, Chen B (2018) Robust color image watermarking technique in the spatial domain. *Soft Comput* 22(1):91–106
54. Sweldens W (1998) The lifting scheme: a construction of second generation wavelets. *SIAM J Math Anal* 29(2)
55. Vaishampayan VA, Sloane N, Servetto S (2001) Multiple description vector quantization with lattice codebooks: design and analysis. *IEEE Trans on Information Theory* 47:1718–1734
56. Wang C, Li X, Yang B (2010) Efficient reversible image watermarking by using dynamical prediction-error expansion, in 2010 IEEE International Conference on Image Processing. p. 3673–3676.
57. Weber G (1993) USC-SIPI image database: Version 4. Dept. Elect. Eng.-Syst., Univ. Southern California, Los Angeles, CA, USA, Tech. Rep. 244
58. Weng S et al (2019) Improved K-pass pixel value ordering based data hiding. *IEEE Access* 7:34570–34582
59. Zheng S, Wang Y, Hu D (2019) Lossless Data Hiding Based on Homomorphic Cryptosystem. *IEEE Transactions on Dependable and Secure Computing*:1

**Publisher's note** Springer Nature remains neutral with regard to jurisdictional claims in published maps and institutional affiliations.



**Ehsan Akhtarkavan** was born in Tehran, Iran, in 1981. He received his B.Sc. degree in hardware computer engineering from I.A.U, Tehran, Iran, in 2004. He was then a network administrator and IT manager at the Academic Center for Education, Culture and Research, Tehran, Iran, until July 2005. He obtained his M.S. degree in computer system architecture from I.A.U, Arak, Iran, in 2007. He received his PhD degree from the School of Electrical and Electronics Engineering, University Science Malaysia, Penang, Malaysia. He is currently Assistant Professor in Department of Computer Engineering, Khatam University, Tehran, Iran and Computer Engineering Researcher in Pasargad Institute for Advanced Innovative Solutions (PIAIS), Tehran, Iran. His current research interests are in digital image watermarking, multiple descriptions image coding and multiple descriptions video coding.



**Babak Majidi** received the BSc and MSc degrees in computer engineering from University of Tehran, Tehran, Iran, in 2000 and 2003, respectively. He received the PhD degree in computer engineering from Swinburne University of Technology, Melbourne, Australia in 2014. He is currently Assistant Professor in Department of Computer Engineering, Khatam University, Tehran, Iran and Computer Engineering Researcher in Pasargad Institute for Advanced Innovative Solutions (PIAIS), Tehran, Iran. His main research interests include machine learning, big data analytics, computer vision and field and service robotics.



**Mohd Fadzli Mohd Salleh** was born in Bagan Serai, Perak, Malaysia. He received his B.S. degree in electrical engineering from the Polytechnic University, Brooklyn, NY, US, in 1995, the M.S. degree in communication engineering from the University of Manchester Institute of Science and Technology (UMIST), Manchester, UK, in 2002, and the Ph.D. degree from the University of Strathclyde, Glasgow, UK, in 2006. He was a Software Engineer with the Department of Research and Development, Motorola Penang, Malaysia, until 2001. Currently, he is an Associate Professor with the School of Electrical and Electronic Engineering, Universiti Sains Malaysia. He has supervised twelve Ph.D. degree students to graduation. His main research interests include source coding and signal processing for application in telecommunications and wireless communication networks.



**Jagdish C. Patra** received his BSc. Eng., MSc. Eng. and PhD degrees, all in Electronics and Communication Engineering, from India in 1978, 1989 and 1996, respectively. Currently, he is serving as a Senior Lecturer at Swinburne University of Technology, Melbourne, Australia. Prior to this job, he worked as a faculty member in different universities in India and Singapore. He visited, as visiting professor, to Technical University, Delft, The Netherlands; University of Tampere, Finland; Iwate Prefectural University, Japan, and HEIG-VD, Switzerland. His major research areas are intelligent signal and image processing using artificial neural networks and evolutionary computing techniques. In addition, he has carried out research work in the areas of modelling and characterization of complex systems. Jagdish has published more than 140 research papers in reputed International Journals and top-tier International Conferences. Some of his publications have been highly cited. He has served as a reviewer for several IEEE Transactions and other international Journals.